



ELSEVIER

Contents lists available at ScienceDirect

Micro and Nano Engineering

journal homepage: www.journals.elsevier.com/micro-and-nano-engineering

Research paper

The design and performance of hydrogen-terminated diamond metal-oxide-semiconductor field-effect transistors with high k oxide HfO₂Chi Sun^{a,b}, Tingting Hao^{a,b}, Junjie Li^{a,b,c}, Haitao Ye^{d,*}, Changzhi Gu^{a,b,*}^a Beijing National Laboratory for Condensed Matter physics, Institute of Physics, Chinese Academy of Sciences, Beijing 100190, China^b School of Physical Sciences, CAS Key Laboratory of Vacuum Physics, University of Chinese Academy of Sciences, Beijing 100049, China^c Songshan Lake Materials Laboratory, Dongguan, Guangdong 523808, China^d School of Engineering, University of Leicester, Leicester LE17RH, UK

ARTICLE INFO

Keywords:

H-diamond
MOSFET
high-k
Normally-off

ABSTRACT

The hydrogen plasma treatment of single crystal diamond was carried out by microwave plasma chemical vapor deposition equipment, and the normally-off hydrogen-terminated diamond field-effect transistors (FETs) with different gate lengths were prepared by atomic layer deposition (ALD) which deposited HfO₂ as gate oxide. We systematically investigated the influence of hydrogen treatment duration, gate length, channel length and gate oxide material HfO₂ on the hydrogen-terminated diamond FETs. Results show that the HfO₂ gate oxide allows the fabricated FETs to exhibit a normally-off characteristic, which is advantageous for the practical application of power devices. The drain-source current, threshold voltage, subthreshold swing, and I_{on}/I_{off} of the fabricated diamond FETs with gate length of 5 μm are 11 mA/mm, -2.9 V, 3 mS/mm, and 10⁶, respectively. With the increase of the gate length (L_g = 5 μm, 20 μm, 50 μm), the drain current density, threshold voltage, and transconductance of the devices decrease, which is due to the higher channel resistance and inhomogeneity of the hydrogen surface termination.

1. Introduction

Diamond offers many outstanding physical properties such as wide band-gap energy, high breakdown field, high thermal conductivity, large carrier saturation velocity, low dielectric constant and high carrier mobility, which makes it very attractive for high-temperature, high-voltage and high-power electronic device applications [1–3]. Diamond can be modified from insulating (intrinsic diamond) to semi-conductive by doping boron (p-type) or phosphorous (n-type). However, the ionization energies of boron acceptors (0.37 eV) and phosphor donors (0.58 eV) are too high to activate carriers at room temperature (RT) which limits the wider applications of diamond in devices [3]. Landrass and Ravi found that as-grown diamond surfaces possess high p-type surface conductivity which was generated by hydrogen termination of the surface [4]. This result can also be obtained by exposing diamond to a hydrogen plasma. Hydrogen-terminated diamond surface is p-type conductive which can generate hole carriers at a concentration of approximately $1 \times 10^{13} \text{ cm}^{-2}$ [5,6]. Unfortunately, this surface conductivity is unstable when the samples overheats or the environment becomes vacuum [7]. Some other researchers discovered that the adsorption of NO₂ or O₂ on diamond surface increased the surface hole

concentration which improves the surface conductivity further [8]. Various physical models have been proposed to explain this intriguing phenomenon but the responsible mechanism is still controversial [9,10]. Despite this, diverse diamond devices have been fabricated by using hydrogen-induced surface conductivity which have exhibited excellent device performance. [11–14]. This p-type conductive layer exists not only in single-crystal diamond but also in polycrystalline diamond. Obviously, single-crystal diamond will offer better electrical properties than polycrystalline diamond due to less grain boundaries and high purity.

Some researchers have reported different high dielectric constant oxides such as HfO₂, Al₂O₃ and TiO₂ for preparing hydrogen-terminated diamond metal-oxide-semiconductor field effect transistors (MOSFETs) with good performance. However, their works on single crystal diamond FETs were mainly focused on depositing high dielectric constant (high-k) gate dielectric materials [15–17], few systematic studies on the regularity of one type gate dielectric material have been reported. In order to understand the insight of the influence of hydrogen surface termination on diamond MOSFETs (HfO₂ as gate oxide), we design different device structures and the effects of hydrogen treatment duration, gate length, and channel length on the device performance

* Corresponding author at: Beijing National Laboratory for Condensed Matter physics, Institute of Physics, Chinese Academy of Sciences, Beijing 100190, China.

E-mail addresses: haitao.ye@leicester.ac.uk (H. Ye), czgu@iphy.ac.cn (C. Gu).<https://doi.org/10.1016/j.mne.2020.100046>

Received 31 August 2019; Received in revised form 27 December 2019; Accepted 6 January 2020

2590-0072/© 2020 The Authors. Published by Elsevier B.V. This is an open access article under the CC BY-NC-ND license (<http://creativecommons.org/licenses/by-nc-nd/4.0/>).

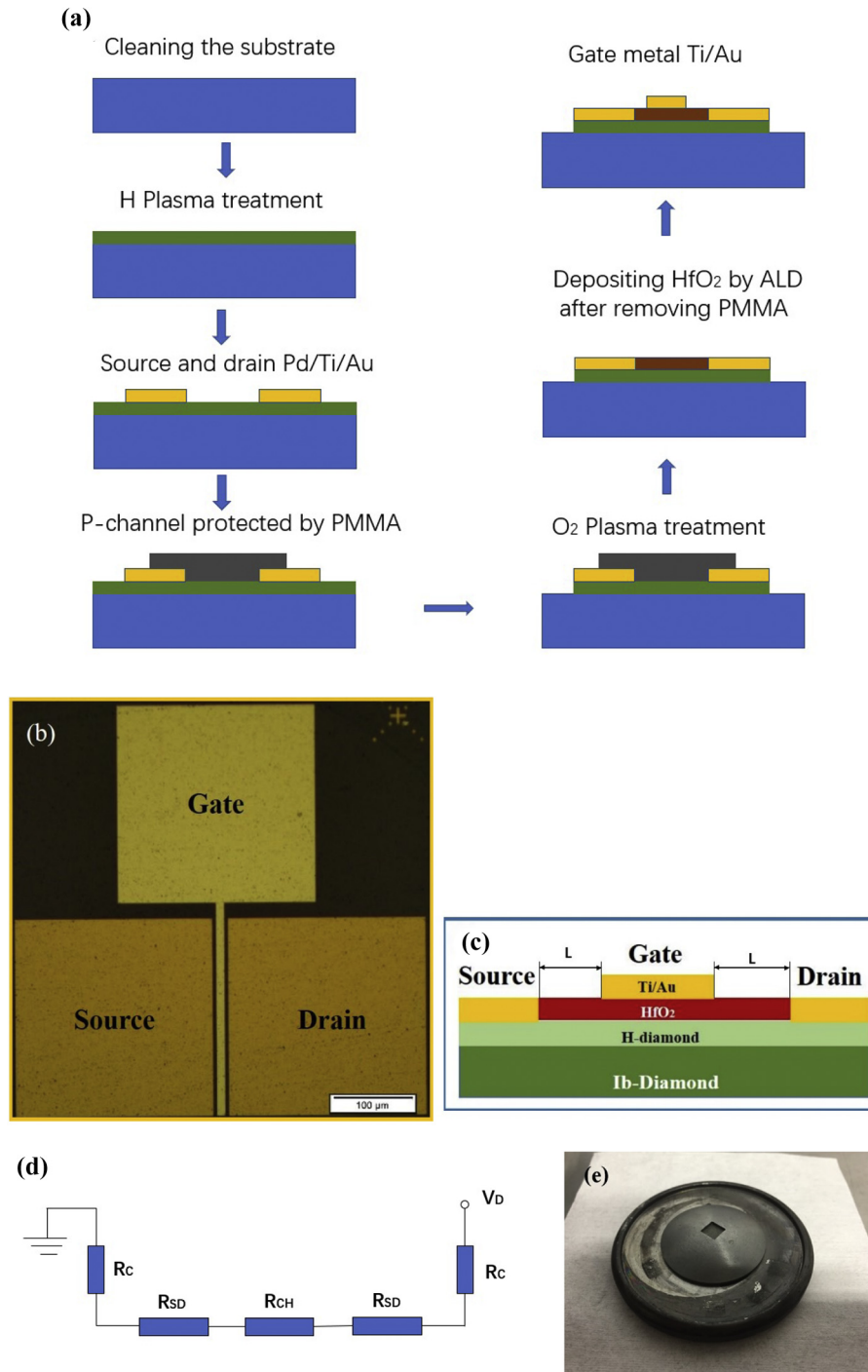


Fig. 1. (a) Fabrication routine for planar H-diamond MOSFETs. (b) Optical micrograph of the device with 10 μm gate length. (c) Schematic cross-sectional structure of the device. (d) The equivalent circuit diagram of the device. (e) The structure of the holder.

are investigated in this paper. The possible physical mechanism responsible for the observed phenomena is also discussed.

2. Experimental

Fig. 1 (a) shows the fabrication processes of H-terminated diamond MOSFETs. The diamond samples for this experiment were (001) single-crystal diamond ($3 \times 3 \times 0.3 \text{ mm}^3$) with extremely low N concentration ($< 1 \text{ ppm}$) and B concentration ($< 0.05 \text{ ppm}$) which were purchased from Element Six (UK). Before the device fabrication, the single-crystal diamond samples were boiled in acid mixed solution

which contains equal portions of HNO_3 and H_2SO_4 at $200 \text{ }^\circ\text{C}$ for 4 h in order to remove any surface nondiamond contamination. After this process the diamond surface was highly insulating [15]. Then the cleaned diamond sample was put into a microwave plasma chemical vapor deposition (CVD) chamber for hydrogenation treatment. In order to fix the small samples we fabricated a special holder for them. The material of the holder is Mo and the structure of the holder is shown in Fig. 1(e). The square inside is $5 \text{ mm} \times 5 \text{ mm}$, where we put the sample. The flow rate of H_2 gradually increased to 400 sccm, the working pressure was 60 Torr, substrate temperature was around $900 \text{ }^\circ\text{C}$ and microwave power was 2 kW. The sample was cooled down in hydrogen

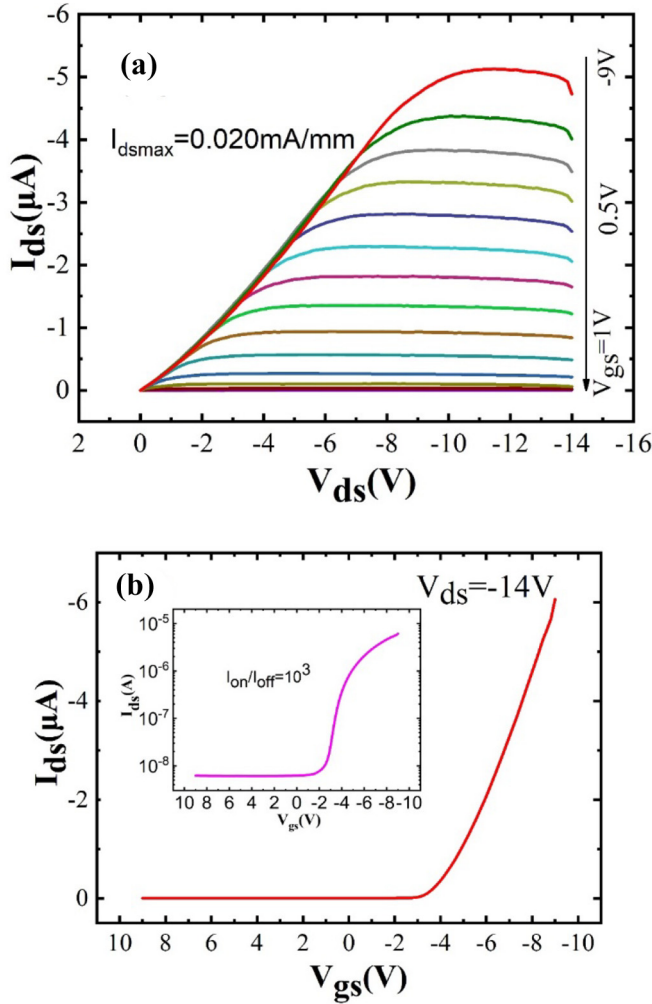


Fig. 2. (a) I_{ds} - V_{ds} output characteristic curve and (b) trans-characteristic curve of the planar H-diamond FET with channel length 20 μm , H process time 10 min. The inset is on a log-scale.

atmosphere and the process duration was set to be 5 min, 10 min, 15 min, respectively. Afterwards, for FET device patterning on the diamond sample, an e-beam lithography technique and an electron beam evaporation (EB) technique were used to prepare the source and drain electrodes (Pd/Ti/Au 10 nm/10 nm/80 nm). The photoresist used in this experiment was PMMA (polymethyl methacrylate) which was a positive electron resist and had a high resolution. We spin coat another water-soluble conductive adhesive on PMMA, which can tackle the challenge of the insulated substrate. The deposition rate for EB process was 0.5 nm/s which was in favor of growing high quality films. Metal Pd could form better ohmic contact with hydrogen-terminated diamond which helped to improve measurement accuracy [16]. After lift-off, we spin coat another PMMA on the sample and used the e-beam lithography technique to form a mask which was used to protect hydrogen surface. Then, the sample was put into a reactive ion etch system (RIE) for achieving insulated O-terminated surface at the non-channel surface. 30 nm HfO_2 gate oxide was deposited by ALD on the whole diamond sample surface at 110 $^{\circ}\text{C}$. Low deposition temperature was chosen to protect the surface hydrogen and stabilise the performance of the devices [17]. The precursor was $\text{Hf}(\text{Net}_2)_4$ with water as the oxidant. The pulse and exposure duration were 15 ms and 60 s, respectively. After that, the sample was spin coat another 200 nm PMMA, we fabricated gate metal (Ti/Au 10 nm/80 nm) with different gate lengths by the same method. After the above steps as shown in Fig. 1(a), the fabricated H-diamond MOSFETs are ready for measurement. Fig. 1 (b)

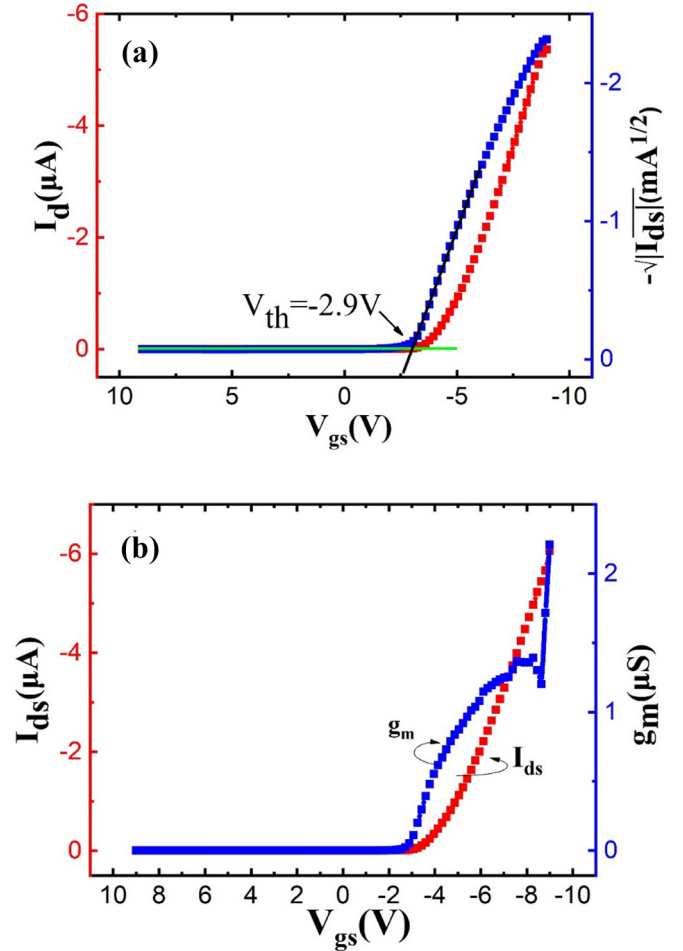


Fig. 3. (a) $-\sqrt{I_{ds}} \sim V_g$ curve and (b) $g_m \sim V_g$ characteristics of the planar H-diamond MOSFET with 20 μm channel length and 10 min H process time.

shows the optical micrograph of the device of the device with 10 μm gate length. Fig. 1 (c) represents the schematic cross-sectional structure of the device, and Fig. 1 (d) demonstrates the equivalent circuit of the device.

3. Discussion

Figs. 2 (a) and (b) show the direct current (DC) output performance and the transfer characteristic, respectively for the fabricated MOSFETs with 20 μm channel length, 250 μm gate width and 10 min H process time. It can be seen that this planar H-diamond MOSFET has a p-type channel. When the gate voltage reaches -9 V , $I_{ds\text{max}}$ and R_{on} will be 0.02 mA/mm and $4.52 \times 10^5 \Omega\text{-mm}$. Transistors have two important parameters, i.e. transconductance (g_m) and threshold voltage (V_{th}). The transconductance reflects the control capability of the gate-source voltage to the drain current, which is an important indicator to characterize the amplification capability of the MOS transistor. The threshold voltage means the transistor has just turned on, which can be affected by the work function of gate electrodes, gate oxide material, and thickness of gate oxide, etc.

Fig. 3 (a) shows the threshold voltage of this device is -2.9 V , which indicates it is a normally-off p-type device. The reason why the device is normally-off is probably the large difference of work function between gate metal Ti (4.33 eV) and H-diamond (4.9 eV). Meanwhile, the hole gas on the H-diamond is very weak, during devices fabrication it could be reduced. Thus, the gate can deplete hole in the channel without gate bias [18,20]. The drain current is lower than other

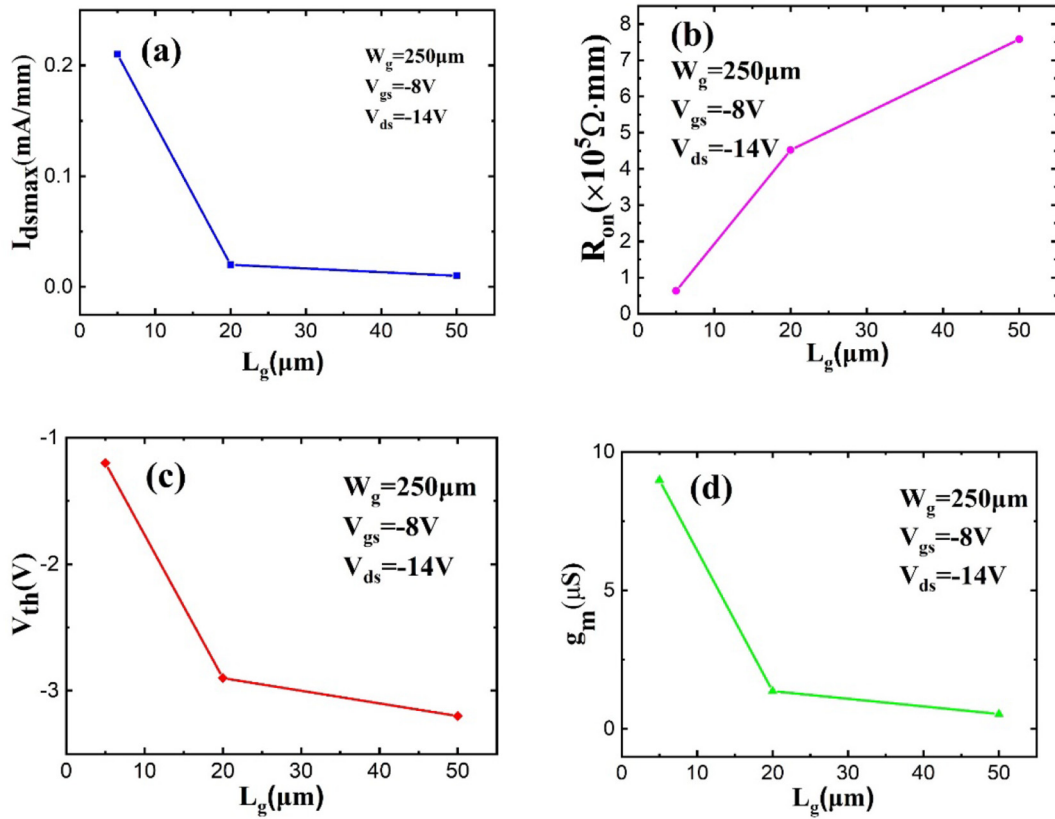


Fig. 4. The influences of gate length on the electronic properties of the planar H-diamond MOSFETs with H process time 10 min, gate width = 250 μm , $L_g = 5 \mu\text{m}$, 20 μm , and 50 μm , respectively. (a) $I_{ds\text{max}} \sim L_g$, (b) $R_{on} \sim L_g$, (c) $V_{th} \sim L_g$ and (d) $g_m \sim L_g$.

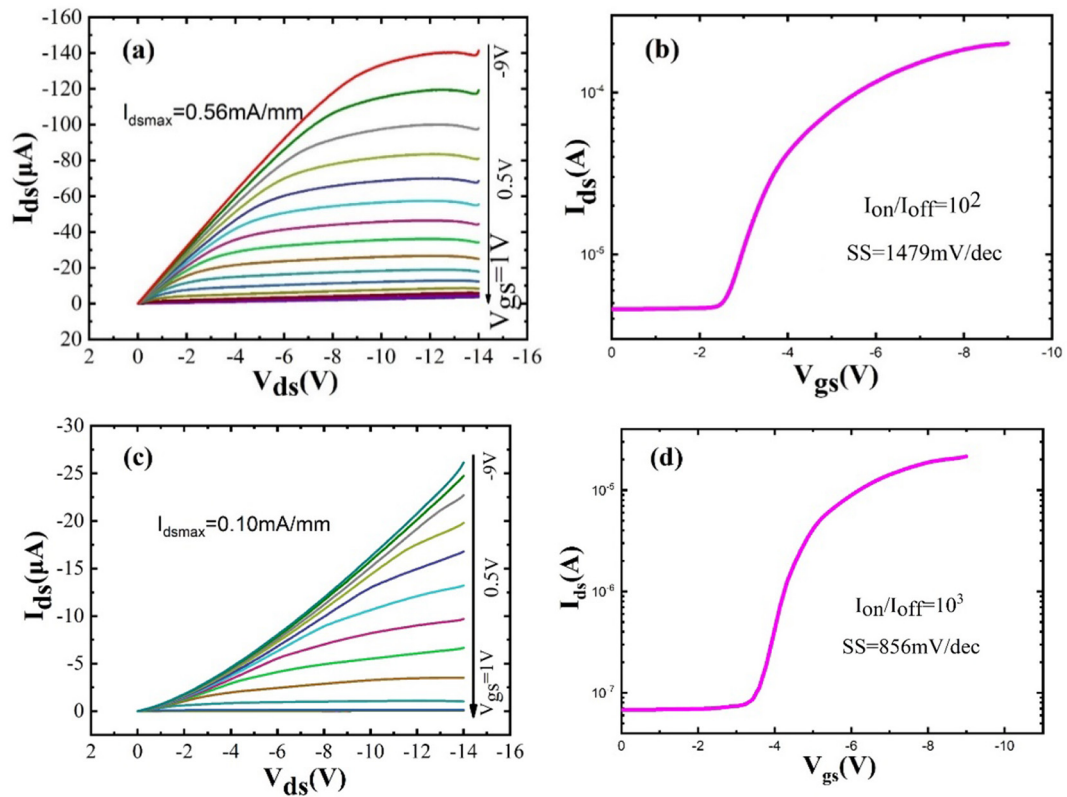


Fig. 5. Output characteristic curves and trans-characteristic curves of the planar H-diamond MOSFETs with the same gate width 250 μm and channel length 30 μm , but different hydrogen treatment time. (a) output characteristic for samples with 15 min hydrogen treatment, (b) transfer characteristic for samples with 15 min hydrogen treatment, (c) output characteristic for samples with 5 min hydrogen treatment and (d) transfer characteristic for samples with 5 min hydrogen treatment.

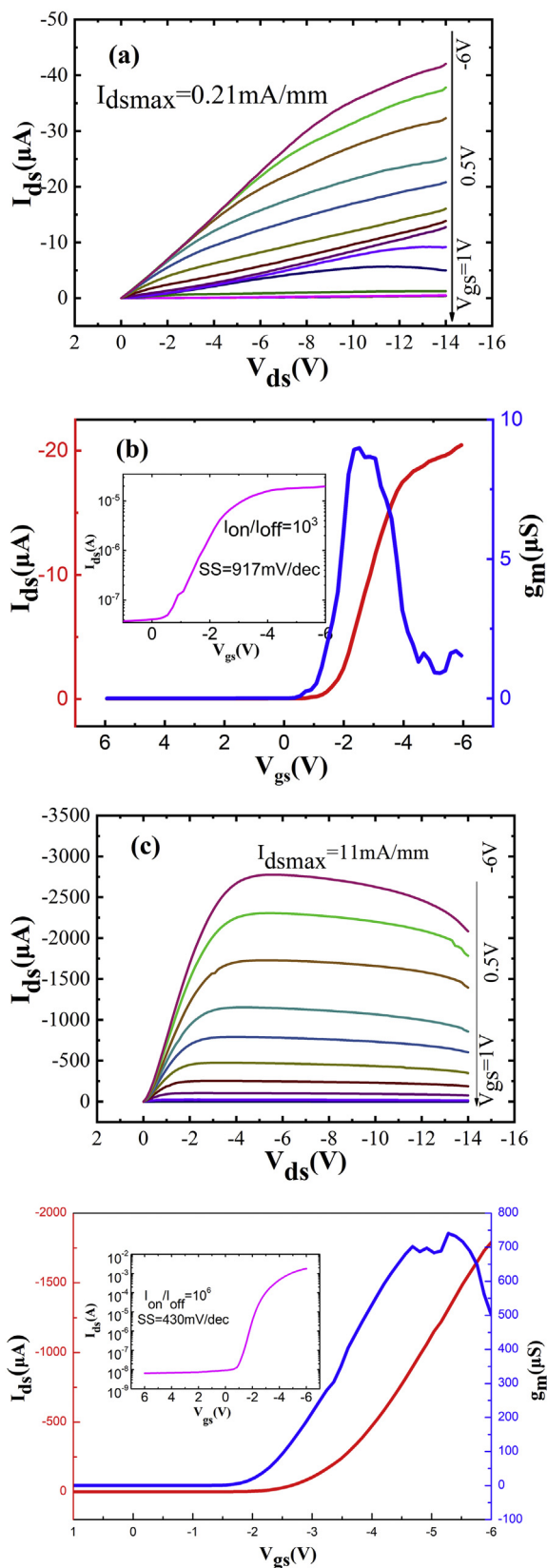


Fig. 6. The output characteristic curves and transfer characteristic curves of the H-diamond MOSFETs (fixed 5 μm gate length, 250 μm gate width and 10 min hydrogen treatment time) with 5 μm space between source/drain and gate (a-b) and with 0.2 μm space (c-d).

reported MOSFETs which have the same gate length but using $Al_2O_3(AlD)/LaAlO_3(SD)$ as gate oxide material [19]. However, the device in our experiment has a low V_{th} , which makes it easier to be turned on. In addition, diamond devices made by the gate oxide material such as CaF_2 , AlN and Al_2O_3 were normally-on [21,23,24]. This fabricated device has a normally-off characteristic which is necessary for practical applications of power devices [22].

To investigate the effect of gate length on the device performance, we obtained representative parameters (R_{on} , V_{th} , I_{dsmax} , g_m) by comparing the device performance of H-diamond FETs with a fixed gate width at 250 μm and a fixed hydrogen treatment duration for 10 min, but with various gate lengths at $L_g = 5$ μm, 20 μm, and 50 μm, respectively. The corresponding curves are shown in Fig. 4.

It can be seen from Fig. 4 that with the increase of gate length, I_{dsmax} , V_{th} and g_m decrease, whilst R_{on} increases from $6.35 \times 10^4 \Omega\text{-mm}$ to $7.58 \times 10^5 \Omega\text{-mm}$. However, there is no linear relationship between R_{on} and the gate length, which indicates that the hole density on the H-diamond surface was inhomogeneous. Furthermore, in the power device MOSFETs, higher R_{on} means higher power consumption of the device. As we know, R_{on} is mainly made up of resistance between source/drain with gate (R_{sd}), source/drain contact resistance R_c , and channel resistance R_{ch} [Fig. 1(d)]. Generally, $R_c \ll R_{ch}$ and $R_c \ll R_{sd}$. R_{sd} and R_c remain the same for different L_g devices. Therefore R_{on} is basically dependent on R_{ch} . Since R_{on} (or R_{ch}) increases as L_g increases [Fig. 4(b)] whilst the voltage remains constant, the current from the source and drain decreases with increasing L_g as seen from Fig. 4(a). In Fig. 4(d), g_m gets less with the increase of gate length. From Fig. 4(c), the change of V_{th} with L_g indicates that L_g can effectively modulate the threshold voltage. The tendency of R_{on} , V_{th} , I_{dsmax} and g_m against L_g is the same with the reported $LaAlO_3/Al_2O_3$ gated H-diamond FETs and Al_2O_3 gated H-diamond FETs [19,22].

Otherwise we investigate the effect of different hydrogen treatment duration on the device performance (output characteristic and transfer characteristic), especially gate control ability, by varying the hydrogen treatment time from 5 min to 15 min as shown in Fig. 5.

The rate of increase of the current below the threshold voltage is characterized by a parameter called the subthreshold slope (SS), which is defined by the relationship:

$$ss = \frac{dV_G}{d(\log(I_d))}$$

V_G is the voltage of gate and I_d is the current from source to drain. The smaller the value of ss , the easier the transition between on and off of the device, the faster the switching speed and the smaller the power loss. However, our device has a low switch ratio and a high subthreshold slope[Fig. 5(b) and (d)], which indicates the control ability of gate is relatively poor.

From Fig. 5 (a) and (c), at the same gate voltage and drain voltage, it can be seen that the output current is large when the hydrogen treatment duration is long, and the maximum output current density is increased by about 5 times if the hydrogen treatment duration increases from 5 min to 15 min. However, the subthreshold slope is reduced from 1400 mV/dec to 856 mV/dec [Fig. 5 (b) and (d)], and the switching ratio is increased by 10 times, indicating that the device has a higher gate control capability for 5 min of hydrogen treatment. This is mainly due to the longer hydrogen treatment duration facilitating the accumulation of more hydrogen-induced hole carriers resulting in larger current between the source and the drain. In the case of the same gate oxide thickness and the device configuration, the control capability of the gate is weakened for samples with 15 min of hydrogen treatment.

In order to further improve the control capability of the gate and increase the drain current, we can reduce R_{on} by reducing R_{sd} in order to increase the drain current. To this end, we have improved the configuration of the device by reducing the distance (from 5 μm to 0.2 μm) between the source/ drain and the gate to reduce the value of R_{sd} . The gate length and the hydrogen treatment time of the H-diamond

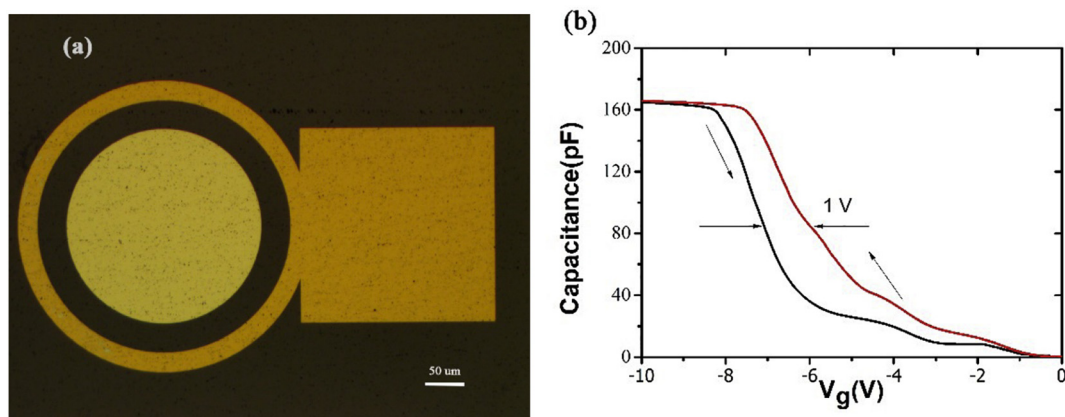


Fig. 7. The optical micrograph of the testing device(a) and the C–V measurement result (b) of the device.

MOSFETs are fixed at 5 μm and 10 min, respectively.

From Fig. 6(a) and (c), we found that for devices with the same gate configuration and the same hydrogen treatment time, the output current increases significantly for the improved devices, mainly because of reduced resistance between the source and the drain. After the improvement, at the gate voltage of -6 V, R_{on} reduces from $6.51 \times 10^4 \Omega\text{-mm}$ to $317 \Omega\text{-mm}$, R_{on} is 2 orders of magnitude smaller than before which indicates resistance between gate and drain(source) is dominant. And also, we find that I_{ds} decreases at high V_{ds} , which mainly caused by small distance between gate and drain. With the increase of V_{ds} , gate voltage is partially shielded which results in reduced I_{ds} . I_{dsmax} increases from 0.17 mA/mm to 11 mA/mm, which is well above the $\text{Al}_2\text{O}_3/\text{O-diamond}$ FET devices of the same configuration [24].

To further explore the key role of HfO_2 , capacity measurement has been completed. Fig. 7(a) shows the optical graph of the testing device. The diameter of the inside circle is $250 \mu\text{m}$. Fig. 7(b) is the measurement result under 5KHz. The C_{max} is almost the same with pre-reported [25], and the dielectric constants of the HfO_2 is calculated to be 11.1. In theory, the flat band voltage(V_{FB}) is -0.45 V which is determined by the work function difference between the H-diamond and Pd. However, the C–V curves of our device shift to left, which indicates large positive fixed charges in the bulk HfO_2 films or the interface between the H-diamond and HfO_2 . Hysteresis behaviors can be found in the C–V curves, which caused by the trapped charges in the bulk HfO_2 films. Considering sputter-deposition(SD) is a good way to improve the quality of HfO_2 film. This result could be mitigated by using sputtering deposition- $\text{HfO}_2/\text{ALD-HfO}_2/\text{H-diamond}$ instead of single ALD- HfO_2 .

Before improvement the maximum transconductance, the subthreshold swing, the switching ratio is $8.98 \mu\text{S}$, 917 mV/dec, 10^3 , respectively. After device optimization, the maximum transconductance, the subthreshold swing, the switching ratio become $740 \mu\text{S}$, 430 mV/dec, and 10^6 , respectively. It can be summarized that the improved device gate control capability is significantly enhanced. Whilst the high k gate dielectric materials plays a key role in determining the diamond power device performance, the device configuration with significantly reduced on-resistance may still dominate the device performance. The combined efforts will need to be considered for the optimal performance for practical power device application.

4. Conclusions

We fabricated the planar H-diamond MOSFETs with 30 nm thick HfO_2 as the gate dielectrics which showed a normally-off P-channel device behavior. The device electrical parameters V_{th} , I_{dsmax} , g_{m} decrease with the increase of the gate length L_{g} . By reducing hydrogen treatment time of the diamond surface and the resistance R_{SD} , we can improve the control capability of the gate. The physical mechanism

responsible for the observed phenomena has been discussed. However, the resultant high subthreshold swing of the device implies its high power loss. The subthreshold swing needs to be further reduced to obtain a device with high output current density and low power loss, for practical applications in integrated circuits with low power loss. We investigated the influence of hydrogen treatment duration, gate length, channel length, on the hydrogen-terminated diamond MOSFETs, which will provide a valuable guidance to the researches on diamond electronics.

Declaration of Competing Interest

The authors declare that they have no known competing financial interests or personal relationships that could have appeared to influence the work reported in this paper.

Acknowledgement

This work was supported by the National Key Research and Development Program of China (Grant Nos. 2016YFA0200400, and 2016YFA0200800), National Natural Science Foundation of China (Grant Nos. 11574369, 61888102, 11674387, 11574385, 11574368), and Key Research Program of Frontier Sciences, CAS (Grant No. QYZDJ-SSW-SLH042). Authors (C.Z. Gu and H.T. Ye) are grateful for the award of UK Royal Academy of Engineering Distinguished Visiting Fellowship.

References

- [1] J. Isberg, High carrier mobility in single-crystal plasma-deposited diamond, *Science* (80-) 297 (2002) 1670–1672, <https://doi.org/10.1126/science.1074374>.
- [2] C.J.H. Wort, R.S. Balmer, Diamond as an electronic material, *Mater. Today* 11 (2008) 22–28, [https://doi.org/10.1016/S1369-7021\(07\)70349-8](https://doi.org/10.1016/S1369-7021(07)70349-8).
- [3] T. Makino, K. Oyama, H. Kato, D. Takeuchi, M. Ogura, H. Okushi, S. Yamasaki, Diamond electronic devices fabricated using heavily doped hopping p + and n + layers, *Jpn. J. Appl. Phys.* 53 (2014), <https://doi.org/10.7567/JJAP.53.05FA12>.
- [4] M.I. Landstrass, K.V. Ravi, Resistivity of chemical vapor deposited diamond films, *Appl. Phys. Lett.* 55 (1989) 975–977, <https://doi.org/10.1063/1.101694>.
- [5] C.E. Nebel, Surface-conducting diamond, *Science* (80-) 318 (2007), <https://doi.org/10.1126/science.1151314> (1391 LP-1392).
- [6] H. Kawarada, Hydrogen-terminated diamond surfaces and interfaces, *Surf. Sci. Rep.* 26 (1996) 205–206, [https://doi.org/10.1016/S0167-5729\(97\)80002-7](https://doi.org/10.1016/S0167-5729(97)80002-7).
- [7] R. Kalish, Diamond as a unique high-tech electronic material: difficulties and prospects, *J. Phys. D: Appl. Phys.* 40 (2007) 6467–6478, <https://doi.org/10.1088/0022-3727/40/20/S22>.
- [8] H. Sato, M. Kasu, Maximum hole concentration for hydrogen-terminated diamond surfaces with various surface orientations obtained by exposure to highly concentrated NO_2 , *Diam. Relat. Mater.* 31 (2013) 47–49, <https://doi.org/10.1016/j.diamond.2012.10.007>.
- [9] F. Maier, M. Riedel, B. Mantel, J. Ristein, L. Ley, Origin of surface conductivity in diamond, *Phys. Rev. B* 85 (2000) 3472–3475, <https://doi.org/10.1103/PhysRevLett.85.3472>.
- [10] A. Denisenko, A. Aleksov, A. Pribil, P. Gluche, W. Ebert, E. Kohn, Hypothesis on the conductivity mechanism in hydrogen terminated diamond films, *Diam. Relat. Mater.* 9 (3–6) (2000) 1138–1142, [https://doi.org/10.1016/S0925-9635\(99\)](https://doi.org/10.1016/S0925-9635(99))

- 00317-9.
- [11] K. Ueda, M. Kasu, Y. Yamauchi, T. Makimoto, M. Schwitters, D.J. Twitchen, S.E. Coe, Diamond FET using high-quality polycrystalline diamond with $f_{\text{sub T}}$ of 45 GHz and $f_{\text{sub max}}$ of 120 GHz, *IEEE Electron Dev. Lett.* 27 (7) (2006) 570–572, <https://doi.org/10.1109/led.2006.876325>.
- [12] J.D. Rameau, J. Smedley, E.M. Muller, T.E. Kidd, P.D. Johnson, Properties of hydrogen terminated diamond as a photocathode, *Phys. Rev. Lett.* 106 (2011) 1–4, <https://doi.org/10.1103/PhysRevLett.106.137602>.
- [13] K. Hiram, H. Sato, Y. Harada, H. Yamamoto, M. Kasu, Diamond field-effect transistors with 1.3 a/mm drain current density by Al_2O_3 passivation layer, *Jpn. J. Appl. Phys.* 51 (2012) 090112, <https://doi.org/10.7567/JJAP.51.090112>.
- [14] K. Wu, M. Liao, L. Sang, J. Liu, M. Imura, H. Ye, Y. Koide, A density functional study of the effect of hydrogen on electronic properties and band discontinuity at anatase TiO_2 /diamond interface, *J. Appl. Phys.* 123 (2018), <https://doi.org/10.1063/1.5002176>.
- [15] J. Shirafuji, T. Sugino, Electrical properties of diamond surfaces, *Diam. Relat. Mater.* 5 (2002) 706–713, [https://doi.org/10.1016/0925-9635\(95\)00415-7](https://doi.org/10.1016/0925-9635(95)00415-7).
- [16] W. Wang, C. Hu, F.N. Li, S.Y. Li, Z.C. Liu, F. Wang, H.X. Wang, Reprint of “palladium Ohmic contact on hydrogen-terminated single crystal diamond film”, *Diam. Relat. Mater.* 63 (2016) 175–179, <https://doi.org/10.1016/j.diamond.2016.01.019>.
- [17] J.W. Liu, M.Y. Liao, M. Imura, Y. Koide, Band offsets of Al_2O_3 and HfO_2 oxides deposited by atomic layer deposition technique on hydrogenated diamond, *Appl. Phys. Lett.* 101 (2012) 1–5, <https://doi.org/10.1063/1.4772985>.
- [18] Y.-F. Wang, X. Chang, X. Zhang, J. Fu, S. Fan, R. Bu, J. Wang, Normally-off hydrogen-terminated diamond field-effect transistor with Al_2O_3 dielectric layer formed by thermal oxidation of Al, *Diam. Relat. Mater.* 81 (2018) 113–117, <https://doi.org/10.1016/j.diamond.2017.11.016>.
- [19] J.W. Liu, M.Y. Liao, M. Imura, H. Oosato, E. Watanabe, A. Tanaka, H. Iwai, Y. Koide, Interfacial band configuration and electrical properties of $\text{LaAlO}_3/\text{Al}_2\text{O}_3$ /hydrogenated-diamond metal-oxide-semiconductor field effect transistors, *J. Appl. Phys.* 114 (2013), <https://doi.org/10.1063/1.4819108>.
- [20] Y. Otsuka, S. Suzuki, S. Shikama, T. Maki, T. Kobayashi, Fermi level pinning in metal-insulator-diamond structures, *Jpn. J. Appl. Phys.* 34 (1995) L551–L554, <https://doi.org/10.1143/jjap.34.l551>.
- [21] M. Imura, R. Hayakawa, E. Watanabe, M. Liao, Y. Koide, H. Amano, Demonstration of diamond field effect transistors by AlN /diamond heterostructure, *Phys. Status Solidi Rapid Res. Lett.* 5 (2011) 125–127, <https://doi.org/10.1002/pssr.201105024>.
- [22] J.L. Hudgins, G.S. Simin, E. Santi, M.A. Khan, An assessment of wide bandgap semiconductors for power devices, *IEEE Trans. Power Electron.* 18 (2003) 907–914, <https://doi.org/10.1109/TPEL.2003.810840>.
- [23] Y.F. Wang, X. Chang, X. Zhang, J. Fu, S. Fan, R. Bu, J. Zhang, W. Wang, H.X. Wang, J. Wang, Normally-off hydrogen-terminated diamond field-effect transistor with Al_2O_3 dielectric layer formed by thermal oxidation of Al, *Diam. Relat. Mater.* 81 (2018) 113–117, <https://doi.org/10.1016/j.diamond.2017.11.016>.
- [24] T. Matsumoto, H. Kato, K. Oyama, T. Makino, M. Ogura, D. Takeuchi, T. Inokuma, N. Tokuda, S. Yamasaki, Inversion channel diamond metal-oxide-semiconductor field-effect transistor with normally off characteristics, *Sci. Rep.* 6 (2016) 31585, <https://doi.org/10.1038/srep31585>.
- [25] J.W. Liu, M.Y. Liao, M. Imura, H. Oosato, E. Watanabe, Y. Koide, Electrical characteristics of hydrogen-terminated diamond metal-oxide-semiconductor with atomic layer deposited HfO_2 as gate dielectric, *Appl. Phys. Lett.* 102 (11) (2013) 112910, <https://doi.org/10.1063/1.4798289>.